Material Model Measurements and Predictions for a Random Pore Poly(ε-caprolactone) Scaffold

T. P. Quinn, T. L. Oreskovic, F. A. Landis, N. R. Washburn

National Institute of Standards and Technology, Boulder, Colorado 80305

Abstract: We investigated material models for a polymeric scaffold used for bone. The material was made by co-extruding poly(ε-caprolactone) (PCL), a biodegradable polyester, and poly(ethylene oxide) (PEO). The water soluble PEO was removed resulting in a porous scaffold. The stress–strain curve in compression was fit with a phenomenological model in hyperbolic form. This material model will be useful for designers for quasi-static analysis as it provides a simple form that can easily be used in finite element models. The ASTM D-1621 standard recommends using a secant modulus based on 10% strain. The resulting modulus has a smaller scatter in its value compared with the coefficients of the hyperbolic model, and it is therefore easier to compare differences in material processing and ensure quality of the scaffold. A prediction of the small–strain elastic modulus was constructed from images of the microstructure. Each pixel of the micrographs was represented with a brick finite element and assigned the Young's modulus of bulk PCL or a value of 0 for a pore. A compressive strain was imposed on the model and the resulting stresses were calculated. The elastic constants of the scaffold were then computed with Hooke's law for a linear-elastic isotropic material. The model was able to predict the small–strain elastic modulus measured in the experiments to within one standard deviation. Thus, by knowing the microstructure of the scaffold, its bulk properties can be predicted from the material properties of the constituents. © 2006 Wiley Periodicals, Inc.* J Biomed Mater Res Part B: Appl Biomater 82B: 205–209, 2007

Keywords: tissue engineering; scaffold; PCL; mechanical properties; hyperbolic model

INTRODUCTION

This work presents empirical and theoretical models of the mechanical response of a porous (ε-caprolactone) (PCL) scaffold to a quasi-statically applied stress. One method to replace injured or missing bone is by use of a biodegradable, synthetic scaffold that can be shaped into the proper geometry before insertion into the body. The scaffold can be cultured with cells *in vitro*, or a bare (or initially seeded) scaffold can be used.[1,2] In both cases the mechanical properties of the scaffold or scaffold/tissue construct must be known in order to ensure that it does not fail mechanically after it is implanted. A typical approach would be for the implant designer to use a finite element model to predict the response of the implant to *in vivo* loads. The mechanical quality of the scaffolds must be assured before they are implanted as well. Here, we present methodology for developing empirical and theoretical material models to address the need for quality assurance, and we demonstrate them using a PCL scaffold as an example.

The mechanical properties of candidate scaffold materials have been measured but usually only the modulus and strength of the material are reported (for examples, see Refs. 3–6). Zein et al.[7] found a good correlation between the yield strength, yield strain, and initial modulus in compression with the porosity of variously structured PCL scaffolds. Ma and Zhang[8] reported the initial modulus and yield strength in compression of poly(L-lactic acid) and poly(D,L-lactic acid-*co*-glycolic acid) scaffolds as a function of polymer concentration. However, these synthetic polymers usually exhibit a nonlinear stress–strain curve that is not easily represented by the initial linear region.

If the microstructure of the scaffold is known it may be possible to predict the mechanical properties of the scaffold. Williams et al.[9] constructed a PCL scaffold with regular geometry (intersecting cylinders) and were able to find a correlation between the compressive modulus and yield strength and the results of a finite element analysis. We intend to show that this technique can be extended to scaffolds with random pore geometries.

Correspondence to: T. P. Quinn (e-mail: quinn@boulder.nist.gov)

In this research, a model form of the stress–strain response of the material in compression has been developed. The model can be used for finite element calculations of the response of an implant made of the scaffold material. We compare the parameters of our model to the secant modulus, which is recommended for rigid cellular plastics by ASTM.[10] Finally we present a method for prediction of the initial modulus based on the microstructure of this random pore scaffold material.

MATERIALS AND METHODS

Scaffold Fabrication

The PCL scaffold used was originally a coextrusion of PCL and poly(ethylene oxide) (PEO) and is described fully in Ref. 11. The PEO is water soluble and can be washed out of the PCL, leaving a network of interconnected pores. The pore structure can be modified by annealing the blend for different cure times. PCL has been shown to be biocompatible with different cell types.[3,11]

In brief, the polymers were blended (initial ratio of PCL to PEO was 1:1 by mass) by use of a twin screw mini-compounder and extruded tubes of polymer were cut into 4 mm diameter cylindrical pieces and annealed in a vacuum oven at 80°C. The copolymer was then molded into square bars $5 \times 5 \times \sim 25$ mm^3 and allowed to anneal at 100°C for 5, 15, 30, and 60 min. The rods were cut into $5 \times 5 \times 5$ mm^3 cubes from which the final $3 \times 3 \times 3$ mm^3 samples were machined. Care was taken so that the final samples came from the center of the 5 mm cubes. Six specimens were made for the four different anneal times. The samples were weighed dry and then suspended in distilled water on a shaker table for 24–48 h to remove the water-soluble PEO. Samples were then dried in a dessicator and weighed again. Porosity resulted in the range of 45–58% (by weight) for all samples. Samples were resuspended in water for 24 h before compression testing.

Mechanical Testing

A table-top, servo-hydraulic, materials-testing machine of 5000 N capacity outfitted with 20 mm diameter platens was used for compression testing. The compression of one face of the sample was recorded with a video microscope with a resolution of about 6 μm per pixel. The load was measured with a ± 100 N load cell with an absolute error of <0.1 %.

The samples were tested in displacement control with the crosshead velocity set to 3×10^{-3} mm/s for a nominal strain rate of 1×10^{-3} s^{-1}. The samples were strained to 20–30% and then unloaded at the same strain rate. The instantaneous recoverable strain is defined here as the difference between the strain just before unloading starts and the strain just as no load is reached. The average strain in the sample was calculated from image correlation of the video. The image correlation was done by selecting a region of 384×288 pixels in the center of the specimen. The region was then subdivided in 32×32 pixel subimages as in Ref. 12. A displacement vector was estimated for each sub-image by maximizing the correlation between the base image (see Figure 1) and the deformed image using bicubic splines to interpolate between pixels. Lines were then fitted to each column (or row) of squares that were vertically (or horizontally) adjacent. Assuming that the strain was uniform, the slopes of these lines were averaged to estimate the normal strains in the sample. To keep the displacements to a few pixels or less, the base image was updated every tenth frame or 21 s. The absolute displacement was maintained by adding
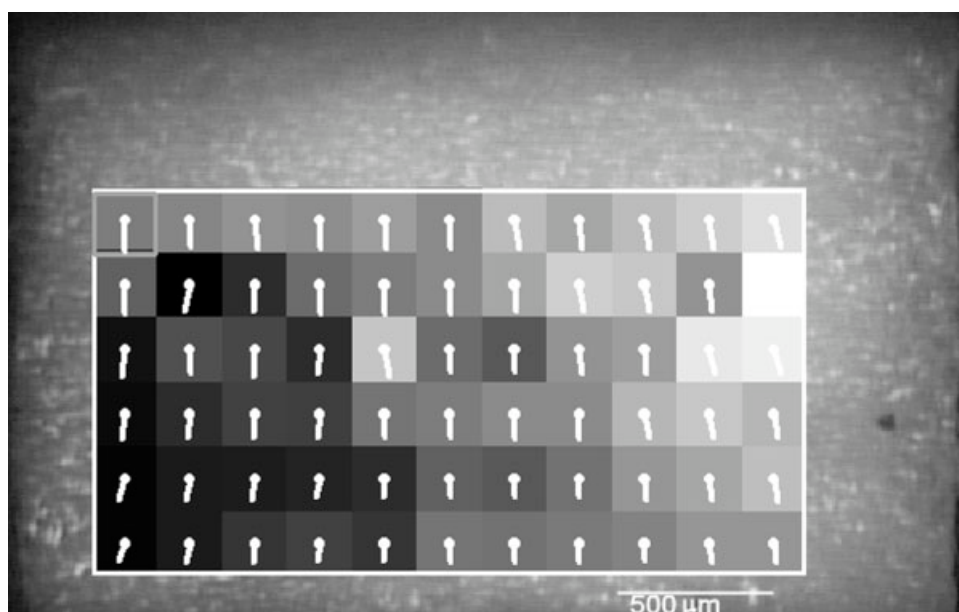

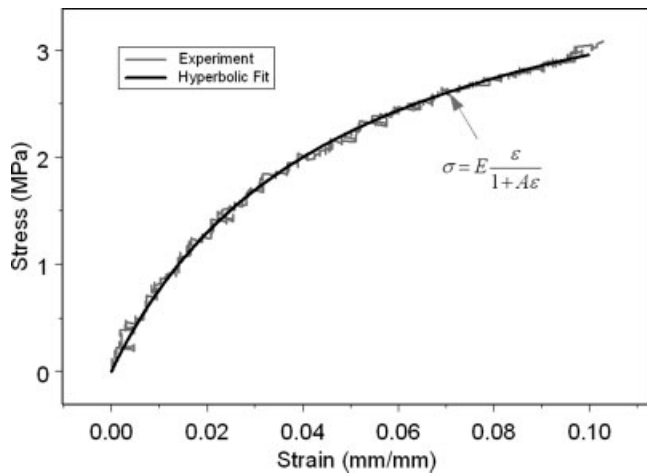**Figure 1.** The displacement vectors superimposed on the subimages.

Figure 2. The stress–strain curve in compression for a PCL scaffold with pore size area of 0.0150 mm^2.

the displacement of subsequent frames to the displacements that were already calculated for the new base image.

The resulting stress–strain (σ–ε) curve was fitted using the method of least squares with a phenomenological model in hyperbolic form: $\sigma = E \frac{\varepsilon}{1 + A\varepsilon}$, where the fitted parameter E is the modulus of the material at small strains, or the initial modulus, and the fitted parameter A is the (dimensionless) strain coefficient. The model asymptotically approaches $\sigma = E/A$ for large strains. For large A, the material approaches an elastic-perfectly plastic state; for small A, the material does not exhibit a linear-elastic region. The secant modulus was also calculated according to Ref. 10. For this material, the secant modulus can be taken as 10 times the stress at 10% strain.

Optical coherence microscopy (OCM)[13] was used to scan the interior of the scaffold samples. Each image of 250 × 250 pixels covers 920 μm^2 with a depth of 4 μm per slice. Five image slices from two scaffold samples from each of the anneal groups were examined by use of OCM. The grey scale OCM images were converted to binary images by use of a threshold after despeckling, and the areas of the pores were measured automatically with image analysis software. Average pore size areas were calculated by averaging the 10 slices for each anneal group. Material property data were compared using a one-way ANOVA test.

Prediction of Initial Modulus

A finite element (FE) model was constructed to predict the initial elastic constant of the material at small strains given the microstructure. The 4 μm cubic pixels from the OCM analysis were used to identify the pores in the material. An automated routine mapped each pixel into an 8-node brick element[14] (3 degrees of freedom per node); each element was assigned the Young's modulus of bulk PCL (386 MPa[15]), or a value of 0 for a pore. A three dimensional model was built up by joining the elements with the corresponding element from the previous OCM slice. Poisson's

TABLE I. Summary of Results of Model Parameters and Pore Size[a]

Pore Size Area (mm^2)	E (MPa)	A	Secant Modulus (MPa)
0.00027 ± 0.00008[b]	135 ± 91	23 ± 25	42 ± 5[c]
0.0019 ± 0.0004[b]	89 ± 40	19 ± 9	30 ± 5
0.006 ± 0.001[b]	122 ± 60	21 ± 13	38 ± 6
0.016 ± 0.002[b]	144 ± 59	30 ± 18	36 ± 5

[a] E, A and the secant modulus were calculated from the stess–strain curves of six samples for each pore size. Two of those samples were mapped with OCM to give the pore size area.
[b] The pore sizes were significantly different with $p < 0.0001$.
[c] Significantly different $p < 0.05$ from the secant modulus of 0.00194 pore size sample. No other material properties showed significance.

ratio for bulk PCL was taken to be 0.3. The equations solved in the FE analysis are those of linear elasticity for small strain theory: here we make the assumption that, at small strains, E (the initial modulus in our empirical model) can be predicted using small strain theory and linear-elastic material properties. To make the approximation, a compressive strain was imposed on the model, and the resulting stresses were calculated. The initial modulus of the sample was then calculated using Hooke's law for a linear-elastic, isotropic material. A paired t-test was used to compare the FE model-predicted E for a sample to the E measured for that sample experimentally. FE models were generated for four samples, one per annealing time.

RESULTS

The PCL samples show a nonlinear response to the applied stress (Figure 2). The hyperbolic fit was able to approxi-

Figure 3. The material map (a 1 mm × 1 mm slice) for the finite element model of the porous PCL scaffold. Black indicates a pore.
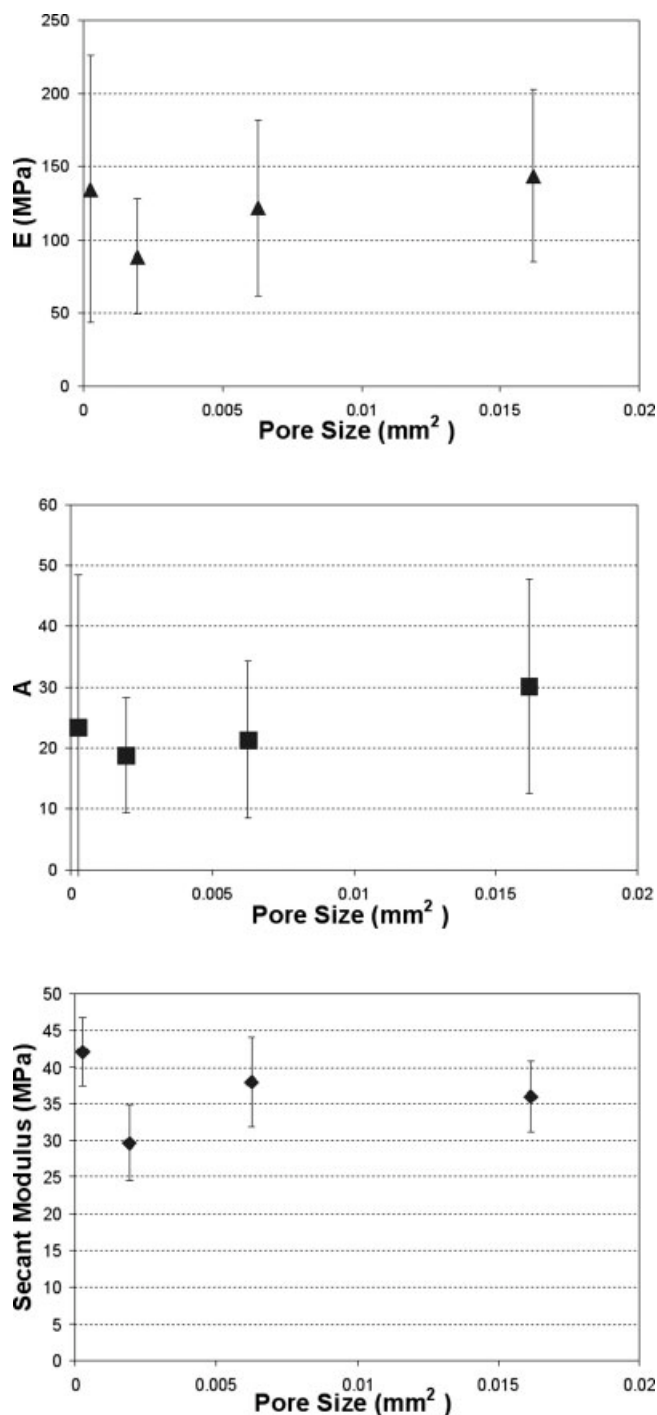
Figure 4. The model parameters and secant modulus as a function of pore size.

icant differences (Figure 4 and Table I). The smallest pore size, 0.00027, showed the highest secant modulus and was a significant increase from the pore size value of 0.00194. The instantaneous recoverable strain was $(8 \pm 2)\%$.

The FE model predicted E of the four samples to a mean paired difference of 11 MPa (the 95 % CI was -85 to 107 MPa) (Table II). There was no significant difference between the model predicted E and the experimentally measured E with $p = 0.74$.

DISCUSSION

Figure 2 shows that the stress–strain curve for PCL cannot easily be approximated linearly up to 10% strain. This hyperbolic material model will therefore be useful for designers of implants made with these types of materials for quasi-static analysis, as it provides a simple form that can easily be used in FE models.[16] The hyperbolic model has the drawback of having relatively large standard deviations in its fitted parameters E and A (up to 67% of the mean for E and up to 108% of the mean for A). Multiparameter models often have large variations in the parameters; see Fung[17] for a discussion of the meaning of the parameter values. The secant modulus (a one-parameter model) offers a much lower variability with the standard deviation, at most, 17% of the mean. It is most likely this reduced variability and ease of computation led to its adoption in the standard.[10] These traits make the secant modulus ideal for use in quality control of scaffold materials.

Maintaining the volume fraction of pores in the material allows the designer of the scaffold to vary the pore size without affecting the elastic properties. For the samples constructed here the pore size could be varied by three orders of magnitude while maintaining the elastic modulus. One would expect that as long as the pore size is small compared with the sample size (as was the case for these sets of samples) the elastic properties would be a function of the volume fraction alone: the samples that have large pores have corresponding thick sections of PCL, and the samples with small pores must have thinner sections of PCL.

The result from the FE model confirms that it is possible to predict the properties of the scaffold if the microstructure of the scaffold is known.[9]

mate the data to an average root mean square (rms) difference of 0.1 MPa, as seen in Figure 2. The results of the modeling and pore size analysis for the four different pore sizes are summarized in Table I. No directionality in pore orientation could be detected in the OCM data (see the material map made with the OCM data in Figure 3). With the single exception of the secant modulus for the smallest pore size, none of the material property data showed signif-

TABLE II. FE-predicted E Compared With Experimentally Predicted E for the Four Samples That Were Modeled

Sample Pore Size Area (mm²)	FE predicted E (MPa)	Experimentally predicted E (MPa)
0.00027	237	256
0.0014	149	48
0.0043	85	110
0.014	79	92

CONCLUSIONS

1. Material models fit to the compressive stress–strain curve for a PCL scaffold material were constructed. A hyperbolic model of the stress–strain curve fitted the data to an rms difference of 0.1 MPa up to 10% strain.
2. Relatively large standard deviations (up to 67% of the mean for E and up to 108% of the mean for A) in the model parameters compared with the means were evident.
3. A secant modulus was also measured and found to have less variability (at most 17% of the mean) therefore making it useful for quality control purposes.
4. Finally, the initial modulus of the material was predicted from the microstructure and the bulk material properties to a mean paired difference of 11 MPa of the experimentally measured value ($p = 0.74$) using a finite element model.

REFERENCES

1. Schantz JT, Teoh SH, Lim TC, Endres M, Lam CX, Hutmacher DW. Repair of calvarial defects with customized tissue-engineered bone grafts. Evaluation of osteogenesis in a three-dimensional culture system. Tissue Eng 2003;9(Suppl 1): S113–S126.
2. Schantz JT, Hutmacher DW, Lam CX, Brinkmann M, Wong KM, Lim TC, Chou N, Guldberg RE, Teoh SH. Repair of calvarial defects with customised tissue-engineered bone grafts. II. Evaluation of cellular efficiency and efficacy in vivo. Tissue Eng 2003;9(Suppl 1):S127–S139.
3. Hutmacher DW, Schantz T, Zein I, Ng KW, Teoh SH, Tan KC. Mechanical properties and cell cultural response of polycaprolactone scaffolds designed and fabricated via fused deposition modeling. J Biomed Mater Res 2001;55:203–216.
4. Engelberg I, Kohn J. Physico-mechanical properties of degradable polymers used in medical applications: A comparative study. Biomaterials 1991;12:292–304.
5. Chu TM, Orton DG, Hollister SJ, Feinberg SE, Halloran JW. Mechanical and in vivo performance of hydroxyapatite implants with controlled architectures. Biomaterials 2002;23:1283–1293.
6. Zhang Y, Zhang M. Three-dimensional macroporous calcium phosphate bioceramics with nested chitosan sponges for load-bearing bone implants. J Biomed Mater Res 2002;61:1–8.
7. Zein I, Hutmacher DW, Tan KC, Teoh SH. Fused deposition modeling of novel scaffold architectures for tissue engineering applications. Biomaterials 2002;23:1169–1185.
8. Ma PX, Zhang R. Microtubular architecture of biodegradable polymer scaffolds. J Biomed Mater Res 2001;56:469–477.
9. Williams JM, Adewunmi A, Schek RM, Flanagan CL, Krebsbach PH, Feinberg SE, Hollister SJ, Das S. Bone tissue engineering using polycaprolactone scaffolds fabricated via selective laser sintering. Biomaterials 2005;26:4817–4827.
10. ASTM. Standard test method for compressive properties of rigid cellular plastics. West Conshohocken: ASTM; 2000. Report No. D 1621-00.
11. Washburn NR, Simon CG Jr, Tona A, Elgendy HM, Karim A, Amis EJ. Co-extrusion of biocompatible polymers for scaffolds with co-continuous morphology. J Biomed Mater Res 2002;60:20–29.
12. Read DT, Cheng Y-W. Proposed standardization effort: Digital-image correlation for mechanical testing. In: Proceedings of the 2001 SEM Annual Conference. Bethel, CT: Society for Experimental Mechanics. pp 365–368. Proceedings of the 2001 SEM Annual Conference, Portland, OR, June 4–6, 2001.
13. Dunkers JD, Cicerone MT, Washburn NR. Collinear optical coherence and confocal fluorescence microscopies for tissue engineering. Opt Express 2003;11:3074–3079.
14. Garboczi EJ. Finite element and finite difference programs for computing the linear electric and elastic properties of digital images of random materials. Gaithersburg, MD: National Institute of Standards and Technology; 1998. pp 4–18. Report No. NISTIR 6269.
15. Dow Chemical Company. Product Information TONE P787 polymer. New Castle, DE: Dow; 2001. p 1.
16. Lawerence KL. ANSYS Tutorial, Release 7.0. City Mission, KS: SDC Publications; 2003. pp 1.23–1.25.
17. Fung YC. Biomechanics. New York: Springer; 1993. pp 347, 348.